

## Chapter 2

# Evaluation

*“Everything has its wonders, even darkness and silence, and I learn, whatever state I may be in, therein to be content.”*

~ Helen Keller

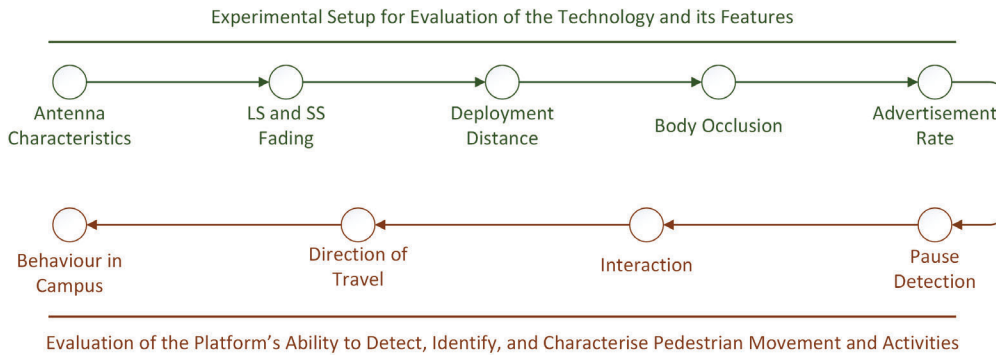
This chapter is aimed at presenting the evaluation of experiments introduced in Chapter 1. The chapter is divided into two sections, related to each evaluation case described in the Methodology chapter. The first set of experiments was conducted to ascertain the viability of the technology, BLE, and its features for measuring pedestrian movement dynamics. This set comprised experiments to evaluate the characteristics of the antenna on the Observer, understand the fading effects of the environment where experiments are conducted, identify optimal deployment distance for the Observer, and assess the effect of the advertisement interval or advertisement rate of the Broadcaster on the measurement of RSSI by the Observer. Through these experiments, ultimately, the technical viability of BLE and the selected hardware platform and the environment was assessed.

The second set of experiments was aimed at evaluating the ability and the accuracy of the Observer in detecting scenarios of heterogeneous pedestrian activities and movement dynamics. The developed system was hence applied to detect pauses in the movement of pedestrians, identify the likelihood of interaction between two pedestrians, ascertain the direction of travel of the pedestrians, and analyse the behaviour of pedestrians through a long-term study on a university campus.

All the outdoor experiments, barring the final one in this chapter, were conducted using a single Observer at the same location, with one or multiple pathways, each 24 metres in length, with five equidistant key points on the pathways – *start*, *approach*, *centre*, *depart*, and *end*, six metres from each other, and a fixed location for deployment of the Observer perpendicular to the *centre* point from all pathways. The decision to conduct experiments in a single location was to create coherent results, obtained from the same building topology. The decision for a 24 metres long pathway was also deliberate as the focus of this study was on micro-level pedestrian dynamics. Moreover, to obtain clear local measurements, that is, observe pedestrian dynamics more accurately, measurement of stronger signals were deemed necessary to facilitate the study.

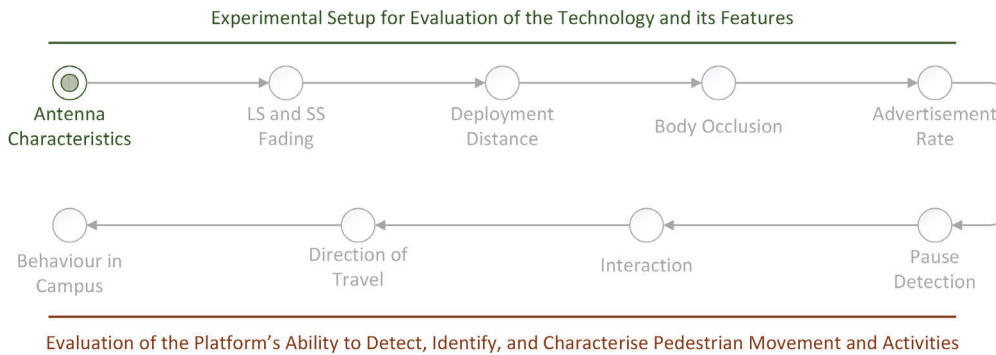
Finally, the date of experiments, span of experiment procedure, number and detail of volunteers involved, and general weather condition at the time of experiments is provided in the respective section of each experiment in this chapter. The orientation of the Observer was the same for all the experiments, as depicted in Figure 1.4 in Section 1.2.2.1 of Chapter 1. The hourly weather information was acquired from the nearby Phoenix Park synoptic weather station by Met Éireann (Éireann, 2023). The weather is 4.6 kms away from the experimental location.

The following figure illustrates the progression of experiments in this chapter. This figure will be used repeatedly to indicate the progress through the different experimental results and associated analysis.



## 2.1 Evaluation of the Technology and its Features

### 2.1.1 Characteristics of the Antenna of the Observer



This experiment was divided into three parts at two different locations, as mentioned in Chapter 1 under the subsection 1.3.2.1. The first part corresponded to the measurements collected in an anechoic chamber where the Observer was rotated, as shown in figure 1.18, such that the signals were emerging from  $0^\circ$ ,  $45^\circ$ ,  $90^\circ$ ,  $135^\circ$ , and  $180^\circ$ , for 3 minutes. This specific resolution was chosen to avoid collecting fewer samples when replicating the experimental setup outdoors. With finer angular resolution than the selected, the resulting RSSI samples will change rapidly as a pedestrian moves along the path. Whereas, valuable details between the chosen angles might be missed with a larger angular resolution than the selected one. The size limitations of the anechoic chamber facility in the university prevented the experiments

from being performed at a distance greater than *3 meters* between the Observer and the Broadcaster.

The second part was conducted in an outdoor environment presented in Figure 1.13. The measurements were first taken radially around the deployed Observer, to replicate the measurements taken in the anechoic chamber, at distances of *3 metres*, *5 metres*, *7 metres*, and *9 metres*, for *3 minutes* each. In this part, a sub-experiment was also conducted to measure the signal strength, the RSSI, at five different locations on two linear pathways *3 metres* and *5 metres* away from the deployed Observer.

Measurements for the experiment conducted in the anechoic chamber were taken on April 4, 2023, starting 14:32 Irish time. Since the measurement was conducted in a noiseless environment, there was no influence of weather conditions or any other external factor. The data collection process in anechoic chamber ended on the same day at 14:45 hours Irish time. The data for the second experiment that measured RSSI at selected angles around the Observer in outdoors were collected between 14:17 hours Irish time and 14:31 hours on February 10, 2023. The weather information during this experiments is described below:

#### At 14:00 hours on February 10, 2023

- **Precipitation (Rain):** 0.0 mm
- **Air Temperature:** 11.8 °C
- **Wet Bulb Temperature:** 10.1 °C
- **Dew Point Temperature:** 8.4 °C
- **Vapour Pressure:** 11.0 hPa
- **Relative Humidity:** 80 %
- **Mean Sea Level Pressure:** 1032.2 hPa

Finally, data for the third, linear pathway, sub-experiment was collected between 11:43 hours and 13:17 hours Irish time on February 1, 2023. Since the experiments spanned over an hour, the weather information presented below is from 12:00 hours and 13:00 hours. The weather information during this experiments are summarised below:

#### At 12:00 hours on February 1, 2023

- **Precipitation (Rain):** 0.0 mm
- **Air Temperature:** 9.4 °C
- **Wet Bulb Temperature:** 7.8 °C
- **Dew Point Temperature:** 6.0 °C
- **Vapour Pressure:** 9.3 hPa
- **Relative Humidity:** 79 %
- **Mean Sea Level Pressure:** 1024.1 hPa

**At 13:00 hours on February 1, 2023**

- **Precipitation (Rain):** 0.0 mm
- **Air Temperature:** 10.0 °C
- **Wet Bulb Temperature:** 8.0 °C
- **Dew Point Temperature:** 5.6 °C
- **Vapour Pressure:** 9.1 hPa
- **Relative Humidity:** 74 %
- **Mean Sea Level Pressure:** 1023.7 hPa

First, each of the three 1-minute segments of measurements were collated and their median was calculated. This collation and calculation was performed for data collected in the anechoic chamber and data collected around the Observer in the outdoor experimental space. The polar charts presented in Figure 2.1 highlights the median RSSI of the entire sample of data for each angle in the anechoic chamber. Similarly, Figure 2.2 presents the median RSSI of the entire sample of data for each angle in the outdoor environment, including the additional data captured at a distance of 5 metres, 7 metres, and 9 metres.

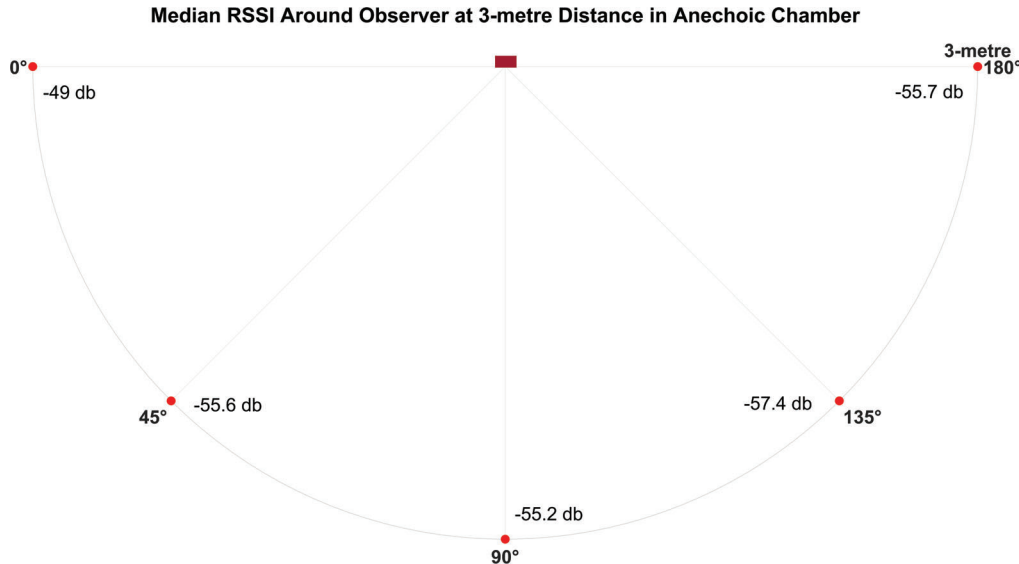


FIGURE 2.1: Median RSSI in Anechoic Chamber for Selected Angles of Measurement

The most striking observation when comparing the median RSSI in the anechoic chamber against the median RSSI at 3 metres deployment distance in the outdoor environment is a significantly improved signal strength in the outdoor environment. Despite being a noiseless environment, the measurements in the anechoic chamber are weaker. While this greater RSSI in the outdoor environment could be an indication of some propagation mechanism acting as a boost on the signals, assessment of RSSI information alone is not sufficient to assert anything about it. To better understand the data, standard deviation and variance were then calculated for both of

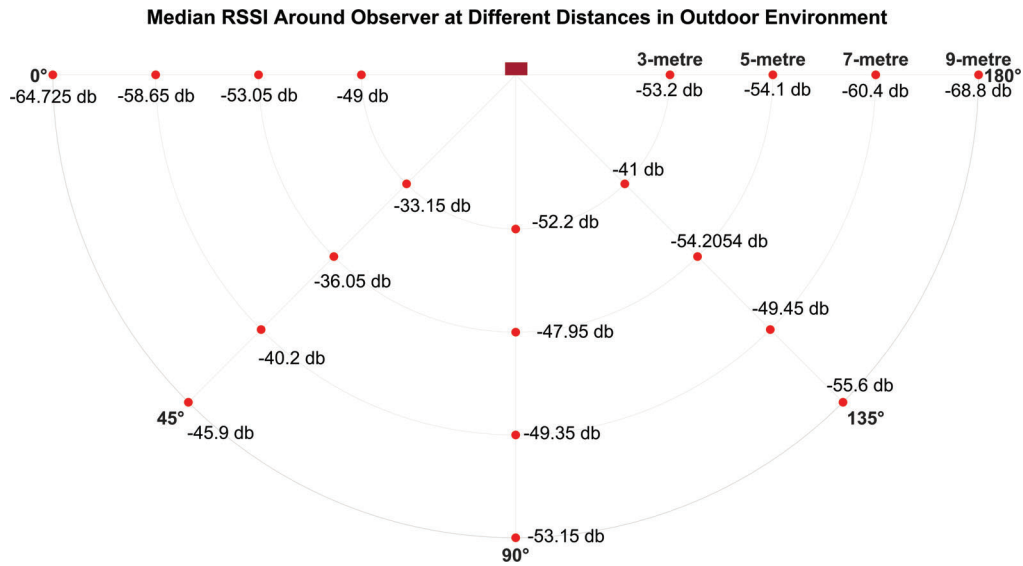


FIGURE 2.2: Median RSSI in Outdoor Environment for Selected Angles and Distances of Measurement

Angle	Anechoic		Outdoor	
	Standard Deviation	Variance	Standard Deviation	Variance
0°	0.1554	0.0241	2.7190	7.3931
45°	0.3552	0.1262	1.9116	3.6544
90°	0.2465	0.0608	3.2216	10.3788
135°	0.2913	0.0848	2.6016	6.7685
180°	0.1595	0.0255	1.0197	1.0397

TABLE 2.1: Comparison of Standard Deviation and Variance of RSSI Collected in an Anechoic Chamber and at 3 Metres Around the Observer in Outdoor Experimental Location

these cases. The outcome is presented in Table 2.1.

Through the calculation of SD and Variance, it was seen that the fluctuations in RSSI were significant in the outdoor measurements compared to those in the anechoic chamber measurements. However, this did not explain the overall increased strength of the signals in the outdoor measurements. It only signified that the spread of values of the collected measurements in the anechoic chamber was lower, indicating that the environment has no external electromagnetic and topological influences which resulted in fewer obstructions in the path of the signal. The increased signal strength in outdoor measurements could be due to several factors. Some of these factors might include constructive interference of reflected signals multipath components (Molisch, 2012) and less absorption of radio waves outdoors than in an anechoic chamber, where, the walls and floor use material that absorbs them (Krchák et al., 2024).

The fluctuations were then plotted using the error bars, depicting the spread of the measurements. The error bars were obtained through MDA technique described in Section 1.4.6 in Chapter 1. The positive and negative errors represented the upper and lower deviation of the RSSI from the median respectively, that is, the extent

of variation above and below the median value. The median value is also plotted on the error bars, denoted by the marker 'x'. These calculations were made on the SMA filtered RSSI, described in Section 1.4.2 of Chapter 1, which are seen on the y-axis. The resulting chart is presented in Figure 2.3. The measurements from the anechoic chamber are shown in green lines and error bars, whereas, red and blue lines and error bars depict the measurements from the outdoor experiment with the deployment distances of 3 *metres* and 5 *metres* respectively. The large error bars in both cases of the outdoor experiments in comparison to the anechoic chamber experiment are a clear indication of the noise produced due to the environmental artefacts.

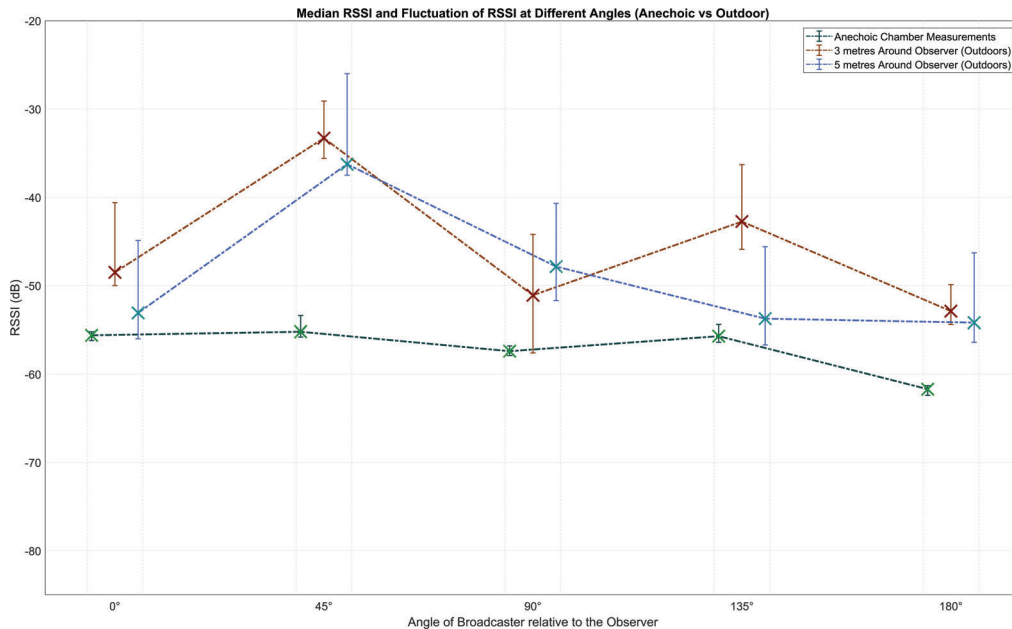


FIGURE 2.3: Span and Median of RSSI Emanating from Selected Angles in an Anechoic Chamber and Selected Angles Around 3-metre and 5-metre Radius Respectively in the Outdoor Environment

The third and final part of this experiment targeted RSSI measurement on linear pathways in front of the Observer, instead of measurements radially around the Observer. Figure 2.4 depicts the median and fluctuation of measurement at *start*, *approach*, *centre*, *depart*, and *end* key points on the pathway (as depicted in figure 1.15) at a distance of 3 *metres* from the Observer coloured in green and the measurements collected radially around the Observer at a distance of 3 *metres* and 5 *metres* in red and blue respectively. It was already intuitive that the signal strength at the extreme ends of the pathway, *start* and *end*, could be low since those locations are the farthest from the Observer on both the linear pathways, which was also confirmed through the RSSI measurements, as seen in Figure 2.4. The difference between the RSSI obtained at each location on 3-metre deployment distance and the RSSI obtained radially around the Observer at 5-metre distance is lesser than the difference between those values at 3-metre pathway and 3-metre radial measurements. While through this it can be inferred that the RSSI measured at each point on 3-metre deployments distance has a closer resemblance to the RSSI measurement radial around the Observer at 5-metres, it adds no value to the experiment objective. These differences are however presented in Table 2.2.

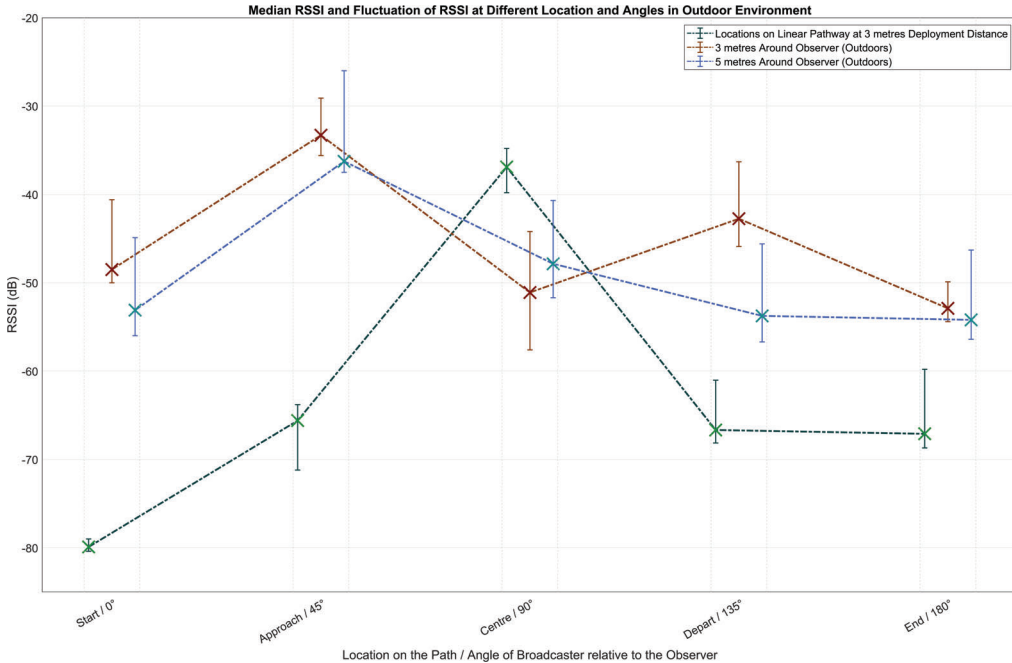


FIGURE 2.4: Span and Median of RSSI Emanating from Selected Key Points and Angled on the Pathway 3-metre Away from the Observer and Around 3-metre and 5-metre Radius Respectively in the Outdoor Environment

Location/Angle	RSSI at 3m, radially around – RSSI at Pathway	RSSI at 5m, radially around – RSSI at Pathway
Start / 0°	31.4	26.8
Approach / 45°	32.3	29.35
Centre / 90°	14.2	10.95
Depart / 135°	23.92	12.92
End / 180°	14.2	12.9

TABLE 2.2: Comparison the Distances between the Median RSSI of Broadcaster Located 5 metres Around the Observer and at Locations on the Pathway Against the RSSI from Broadcaster Located 3 metres Around the Observer

While there was no resemblance between the double hump pattern obtained in the anechoic chamber and at 3 *metres* deployment around the Observer with the RSS pattern obtained at different locations on the pathway, it was noted that the volunteer pedestrian was instructed to stand still at each of those locations. To establish whether or not the double hump pattern appears in the outdoor pathway for this experimental configuration and topology, another condition was tested where the pedestrian was instructed to move along the pathway. Since, the investigation of the movement of the pedestrian will follow in Sections 2.1.3 and 2.1.4, the case of movement was not tested here. However, clear directional sensitivity of the Observer's antenna for BLE signals arriving from 45° and 135° was observed in both the anechoic chamber and at 3 *metres* around the Observer. Therefore, for this particular experimental configuration, there is a likelihood of finding a peak in the collected RSS values of a Broadcaster carried by a pedestrian in motion at an angle of 45°, the *approach* key point or *approach* region, from the plane of the Observer. Also, the error bars in Figure 2.4 showed that the total span of these measurements in both

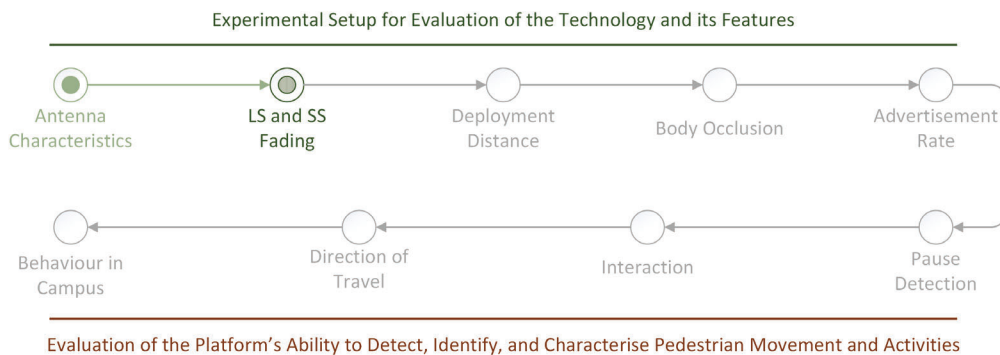
of these cases have overlapping RSS values, suggesting that there could be a likelihood, however small, of another lesser peak in the plot at an angle of 135° or, closer to the *depart* key point.

### Section Summary

The findings from this experiment are useful. One may intuitively think that the peak must be observed when the Broadcaster is directly opposite the Observer. However, as seen in this case, there is a greater likelihood of finding a peak before the *centre* region and a lesser likelihood of finding a second peak after that region when the pedestrian is walking from the *start* region to the *end* region. This demonstrates that any studies or use of this technology to detect the proximity of pedestrians without first investigating the characteristics of the receiver antenna may result in feigned proximity. This will be further elucidated in Section ?? in Chapter ?. The shape of the pattern can also potentially aid in the identification of the direction of a pedestrian simply by observing the pattern of the RSSI and comparing it to the antenna characteristics.

The work presented in this section is part of the publication titled, "Indication of Pedestrian's Travel Direction Through Bluetooth Low Energy Signals Perceived by a Single Observer Device" (Parmar, Kelly, and Berry, 2023b).

### 2.1.2 Large-Scale (LS) and Small-Scale (SS) Fading



Fading underscores the influence of environmental factors in the attenuation of a BLE signal. To understand the effect of the surrounding environment on the location selected for all outdoor experiments, except the last experiment, in this research, both LS and SS fading components were investigated. The measurements used to evaluate both types of fading were acquired for other experiments – LS fading using data acquired from the self-body occlusion experiment described in Section 2.1.4 and SS fading using data acquired from the optimal deployment distance experiment described in Section 2.1.3, both in this chapter. Therefore, the day, time, duration, and weather condition during the experiments will be presented in the respective sections.

### 2.1.2.1 LS Fading

#### Quick Recap

*LS fading:* Also known as Shadowing, it is a type of wireless signal attenuation that occurs due to environmental factors over long distances and correspond to presence of large obstructions in the path of the signals. Described in Section ?? in Chapter ??.

Before calculating the LS fading component, a reference RSSI was obtained for the pair of devices by averaging the measurements at all angles in the anechoic chamber, as described in Section 1.3.2.2 in Chapter 1. The obtained results are:

$$\begin{aligned} RSSI_{ref} &= -57.439 \text{ dB} \\ d_{ref} &= 3 \text{ metres} \end{aligned}$$

These reference values were then used to calculate LS fading through curve fitting. The LS residuals were calculated by assessing the difference between the mean RSSI obtained at five key points to understand the impact of either shadowing or reflection at each of the key points on the pathway.

The calculation of LS fading was performed by comparing the measured RSSI at various locations with the values predicted by a path loss model. Figure 2.5 provides a visual comparison between the measured mean RSSI and the fitted path loss model across five key points: *start*, *approach*, *centre*, *depart*, and *end*. The calculations are also presented in Table 2.3. In the table, it can be observed that the mean RSSI varies significantly between different key points, with the strongest at *centre* (-44.71 dB) and the weakest at *end* (-68.13 dB). Residuals, the difference between mean of the measured RSSI and the predicted RSSI obtained from model fitting, determine if other factors apart from distance attenuate the signals. Table 2.3 also presents significant residuals, varying from -6.25 dB at *end* key point to 7.69 dB at *approach*. Negative residuals in the table signify that the signals are weaker than expected, potentially due to obstacles, shadowing, or interference, suggesting that the model overestimates the signal strength at that location. Negative residuals were observed at *start*, *depart*, and *end* key points on the pathway, with substantially large negative value at *end* key point. Whereas, the positive residual, signifying that the measure RSSI is higher than predicted RSSI, indicates the presence of constructive interference, reflections, or an unobstructed LoS. Positive residual were observed at *approach* and *centre* key points. The Relative Error signifies the percentage deviation of the measured value over the predicted value.

Location	Mean RSSI (dBm)	Fitted RSSI (dBm)	LS Residual (dBm)	Relative Error Percentage (%)
start	-63.26	-61.88	-1.38	-2.23
approach	-47.54	-55.23	7.69	13.92
centre	-44.71	-46.50	1.79	3.85
depart	-57.09	-55.23	-1.86	-3.37
end	-68.13	-61.88	-6.25	-10.10

TABLE 2.3: Large-Scale Fading

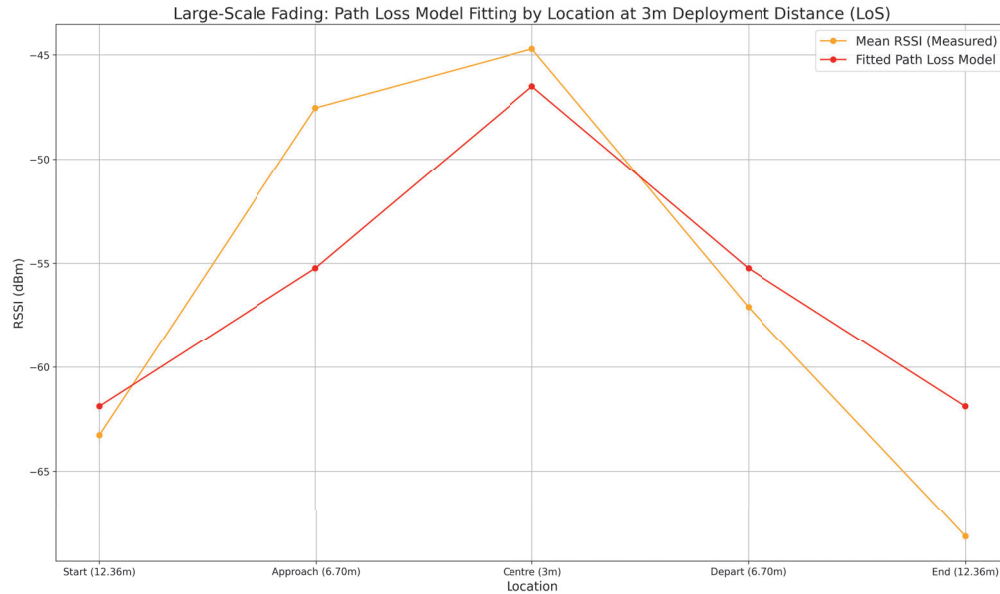


FIGURE 2.5: Comparison of Mean RSSI and Predicted RSSI

### 2.1.2.2 SS Fading

SS fading was analysed by fitting the Rician distribution, described in Section 1.4.11 in Chapter 1, to the deviations of measured RSSI from the mean RSSI at each key point. Figure 2.6 depicts the PDFs of fitted Rician distributions corresponding to the fluctuations caused by multipath propagation at each key point, and the values are summarised in Table 2.4. The Shape parameter,  $K$ , which is used to indicate the dominance of LoS component, is seen highest and substantially large at the *start* key point, signifying the dominance of LoS component. Key points *depart* and *end* corresponded to Rayleigh distribution, indicating the presence of only multipath components. Finally, *approach* and *centre*, with a Shape parameter close to zero, indicated the dominance of multipath components with the presence of some LoS components.

#### Quick Recap

**SS fading:** A type of wireless signal attenuation that refers to rapid fluctuations in signal amplitude, phase, or frequency over short distances or time-periods, typically caused by the interference of multiple signal path, known as multipath propagation. Described in Section ?? in Chapter ??.

Location	Mean RSSI (dBm)	Fitted RSSI (dBm)	Shape Param (K)	Scale Param ( $\sigma$ )
start	-63.26	-45.75	37.18	5.47
approach	-47.54	-53.28	0.20	13.93
centre	-44.71	-57.68	0.14	17.14
depart	-57.09	-60.80	0.00	6.12
end	-68.13	-63.22	0.00	5.04

TABLE 2.4: Small-Scale Fading

The scale parameter, indicating signal fluctuation, was found to be highest at the *centre* key point and least at *end* key point. The scale parameter at *centre* and

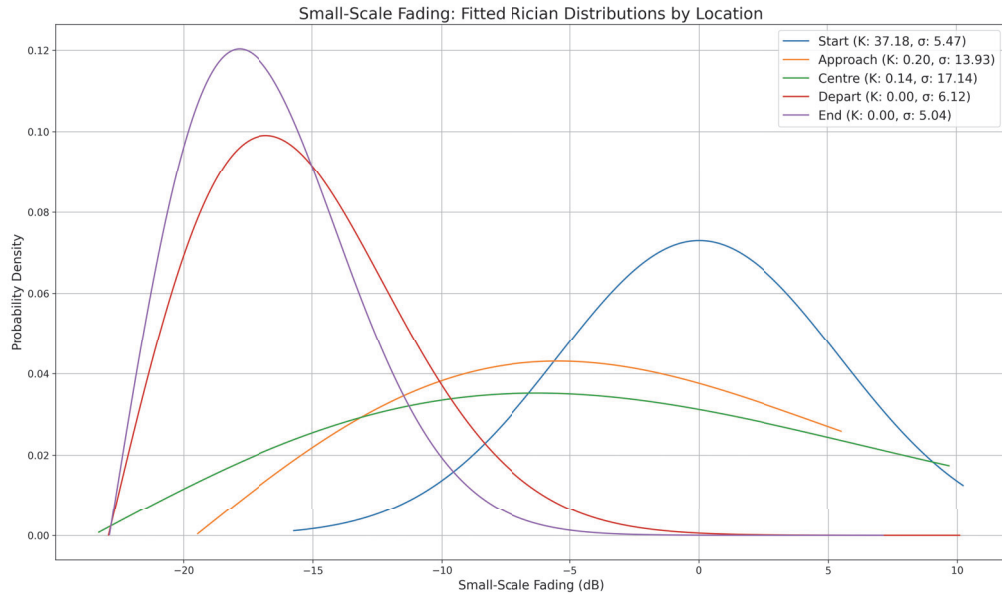
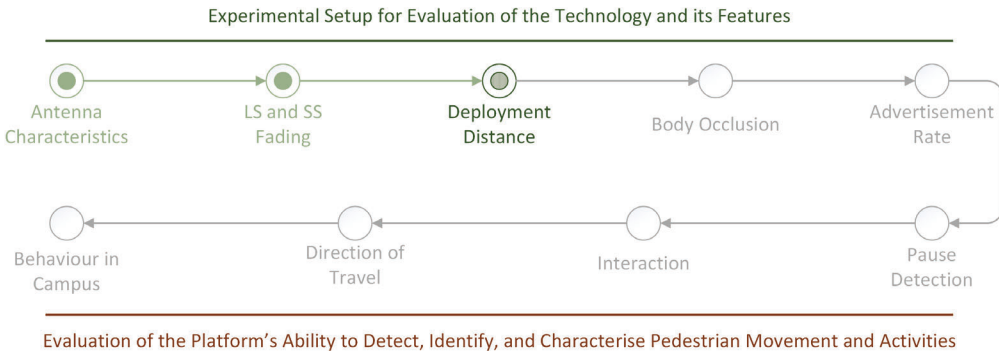


FIGURE 2.6: Rician Distribution Fitting to Deviations at Each key point

approach, as seen in Table 2.4, suggests high fluctuation at these key points, likely due to complex multipath components arising at these locations.

### 2.1.3 Optimal Deployment Distance of the Observer



To assess the optimal deployment distance, 4 candidate distances, 3 metres, 5 metres, 7 metres, and 9 metres were selected. Thus, four paths were marked at those distances from the deployed Observer, each with five key points viz. *start*, *approach*, *centre*, *depart*, and *end*. Two cases, LoS and nLoS, were examined in this experiment. The volunteer pedestrian was instructed to stay stationary at each of those points on each path, one after the other, and measurements were taken in three rounds, each for one minute.

The procedure for this experiment was the same as the one for identifying the antenna characteristics of the Observer, described in Section 2.1.1 in this chapter. However, while the antenna characteristics experiment only used 3 metres and 5

metres deployment distances, this experiment extended the measurement to additionally assess 7 metres and 9 metres deployment distances, as well extended the orientation of the Broadcaster to nLoS case. The measurements date, time, duration, and weather conditions for LoS case were the same as presented in Section 2.1.1 in this chapter. However, measurements for nLoS cases were taken on February 10, 2023 between 12:05 and 14:05 hours Irish time. The weather at 12:00, 13:00, 14:00 hours on the day of this experiment is presented below:

**At 12:00 hours on February 10, 2023**

- **Precipitation (Rain):** 0.0 mm
- **Air Temperature:** 10.7 °C
- **Wet Bulb Temperature:** 9.5 °C
- **Dew Point Temperature:** 8.2 °C
- **Vapour Pressure:** 10.9 hPa
- **Relative Humidity:** 84 %
- **Mean Sea Level Pressure:** 1032.6 hPa

**At 13:00 hours on February 10, 2023**

- **Precipitation (Rain):** 0.0 mm
- **Air Temperature:** 11.2 °C
- **Wet Bulb Temperature:** 9.8 °C
- **Dew Point Temperature:** 8.4 °C
- **Vapour Pressure:** 11.0 hPa
- **Relative Humidity:** 82 %
- **Mean Sea Level Pressure:** 1032.3 hPa

**At 14:00 hours on February 10, 2023**

- **Precipitation (Rain):** 0.0 mm
- **Air Temperature:** 11.8 °C
- **Wet Bulb Temperature:** 10.1 °C
- **Dew Point Temperature:** 8.4 °C
- **Vapour Pressure:** 11.0 hPa
- **Relative Humidity:** 80 %
- **Mean Sea Level Pressure:** 1032.2 hPa

Before delving into the analysis for assessing optimal deployment distance, the restriction of candidate deployment distances to 9 *metres* must be clarified. The selected linear pathway was 24 *metres* in length, irrespective of the distance between the pathway and the Observer. Since the Observer was deployed halfway across the pathway, the farthest locations on each pathways were their respective *start* and *end* key points. The closest distance between the pathway and the Observer was the deployment distance itself, that is the *centre* key point, whereas the farthest distance between the Observer and pathway would be at those farthest points, which can be calculated using Pythagoras theorem, an example of this was presented in Figure 1.19 in Chapter 1.

Based on Pythagoras Theorem, the distance between the Observer and *start* key point can be calculated using the formula expressed in Equation 2.1 as the shortest distances between these points on the pathway for a right-angled triangle.

$$\text{hypotenuse} = \sqrt{\text{base}^2 + \text{perpendicular}^2} \quad (2.1)$$

where:

- *hypotenuse* is the distance between Observer and ‘start’ key point,
- *base* is the distance between ‘start’ point and ‘centre’ point, and
- *perpendicular* is the distance between the Observer and ‘centre’ point on the pathway.

For this experimental case, the value of *base* was 12 irrespective of the deployment distance because the Observer was deployed at the centre of the pathway, whereas *perpendicular* was the deployment distance under test. Using the Equation 2.1, *hypotenuses* for the pathway can be calculated which will be the farthest distance signals will travel to reach the Observer on the respective pathway. This is presented in Figure 2.7, where, aside from candidate distances for this experiment (3 *m*, 5 *m*, 7 *m*, and 9*m*), 11 *metres* deployment distance is also selected for scrutiny.

In the figure, it can be seen that the *hypotenuse* increases with an increase in the deployment distance. However, upon closer inspection, it can be seen that the difference between the *hypotenuse* and respective *perpendicular* is decreasing. The reduction of the difference between them means that the difference in the longest and the shortest distance for the signal to travel is insignificant for the measured length of the respective pathway. That is, if the experimental pathway was 70 *metres* long, then it would have been near the limit of the BLE range and significant differences would still persist. To visualise this, the ratio between these distances is plotted against respective deployment distances. To facilitate reasoning, more candidate deployment distances are selected. Figure 2.8 presents the ratios against deployment distances, with a second y-axis representing the *hypotenuse* or, the distance between *start* key-point and Observer, or, the longest distance for signal to travel on the pathway.

As presented in the figure, the ratio approaches 1 as the deployment distance is increased, signifying that the span of signal travel distance will not vary significantly with increase in deployment distance. Such a situation will prevent any significant trends in the resulting RSSI for inferring pedestrian activities or movement through those measurements. That is, the difference between the shortest distance

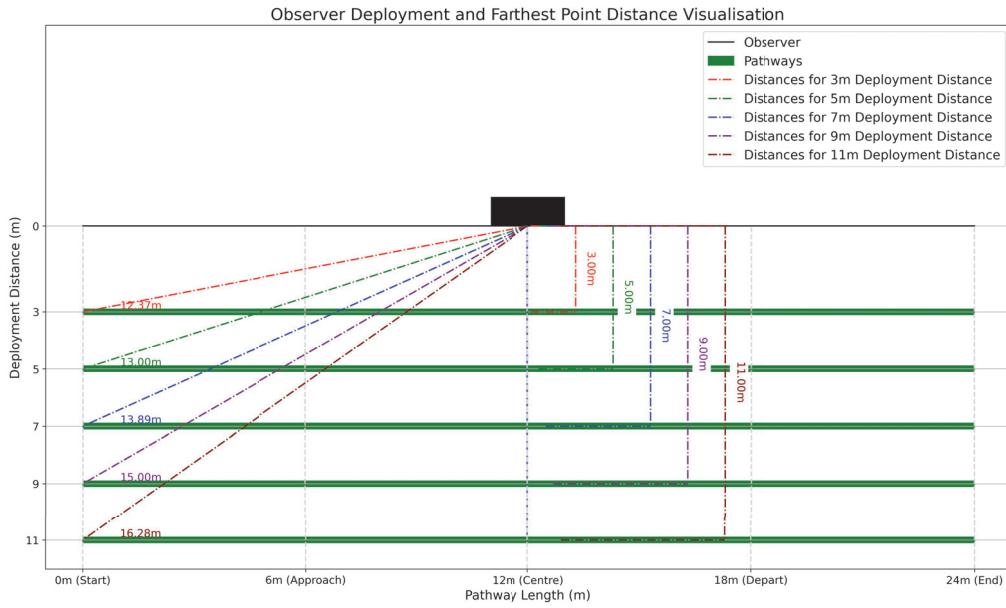


FIGURE 2.7: Visualisation of Distances Between Observer and *Start* Key-point on Different Pathways

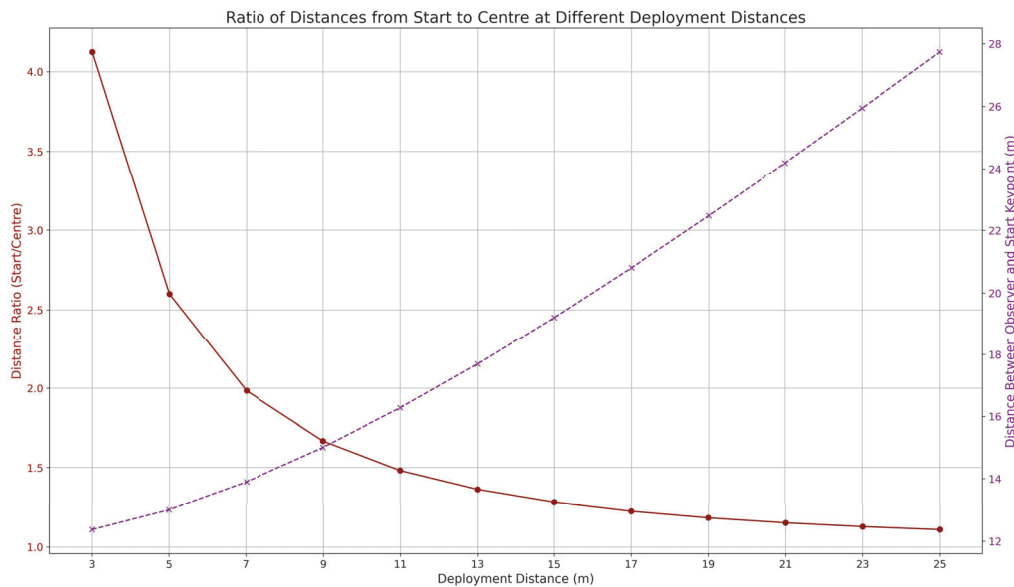


FIGURE 2.8: Ratio of Distance from *Start* to Observer and from *Centre* to Observer at Various Deployment Distances

from Observer to the pathway, viz. the *centre* key point, and the longest distance from Observer to the pathway, viz. *start* and *end* key points reduces as the deployment distance increases. For example, consider two deployment distances, *3-metre* and *15-metre*. The *3 metres* deployment distance pathway will comprise *start*, *approach*, *centre*, *depart*, and *end* key points at a distances of  $\approx 12.37$  metres,  $\approx 6.70$  metres, 3 metres,  $\approx 6.70$  metres, and  $\approx 12.37$  metres respectively from the Observer. Whereas, on the *15-metre* deployment distance, the same key points will be at a distances of  $\approx 19.21$  metres,  $\approx 16.12$  metres, 15 metres,  $\approx 16.12$  metres, and  $\approx 19.21$  metres respectively. The difference between the shortest distances from the Observer, that is the *centre* key point, and key points *start* or *end* in the case of *3-metre* deployment distance is  $\approx 9.37$  metres, whereas, this difference between *centre* key point and *approach* or *depart* key point is  $\approx 3.70$  metres. The same calculation in the case of *15-metre* deployment distance yields respective differences of  $\approx 4.21$  metres and  $\approx 1.12$  metres between *centre* and *start/end* key points and *centre* and *approach/depart* key points. This reduction in the distances of different locations on the pathway from the Observer at higher deployment distances would lead to insignificant pattern changes in the resulting RSSI over the chosen experimental area, which subsequently, will impact detection and identification of pedestrian activity and movement dynamics.

Intuitively, the first approach was to compare the signal strength on each of these paths to assess if the deployment distance results in '*useful*' patterns in the resulting RSSI from the acquired signals. '*Useful*' pattern here implies that the trend in the RSSI contains distinguishable movement that would deviate from what could be caused by fluctuations or artefacts of wireless propagation mechanisms such as reflection. This was performed in phases. First, the RSS values obtained in each of the three rounds of measurement for each location on each path were used to evaluate their respective median signal strength. These medians of all the rounds of measurements at each location on every path were then averaged. This provided a single value representing all of the rounds at each location. The term *averaged median* will be used to refer to this calculated value hereon. Finally, all the averaged medians belonging to a single pathway, or five averaged medians per pathway, were again averaged to calculate a single descriptive value representing the overall signal strength on a path. Through this approach, it was possible to assess not only the overall strength of the signal acquired from a path but, also provide insights into the localised signal strength acquired from a certain location on each of those pathways through the intermediate averaged mean parameter.

Figures 2.9, 2.10, 2.11, 2.12, and 2.13 depict the captured RSS values at *start*, *approach*, *centre*, *depart*, and *end* locations respectively on each of the pathways with their own median values, and the mean of those median values in the case of LoS. In these figures, and the subsequent figure depicting similar parameters in this format, the x-axis, *Instance*, represents the sequence of the acquisition of advertisements which resets to zero at the start of each new deployment distance region.

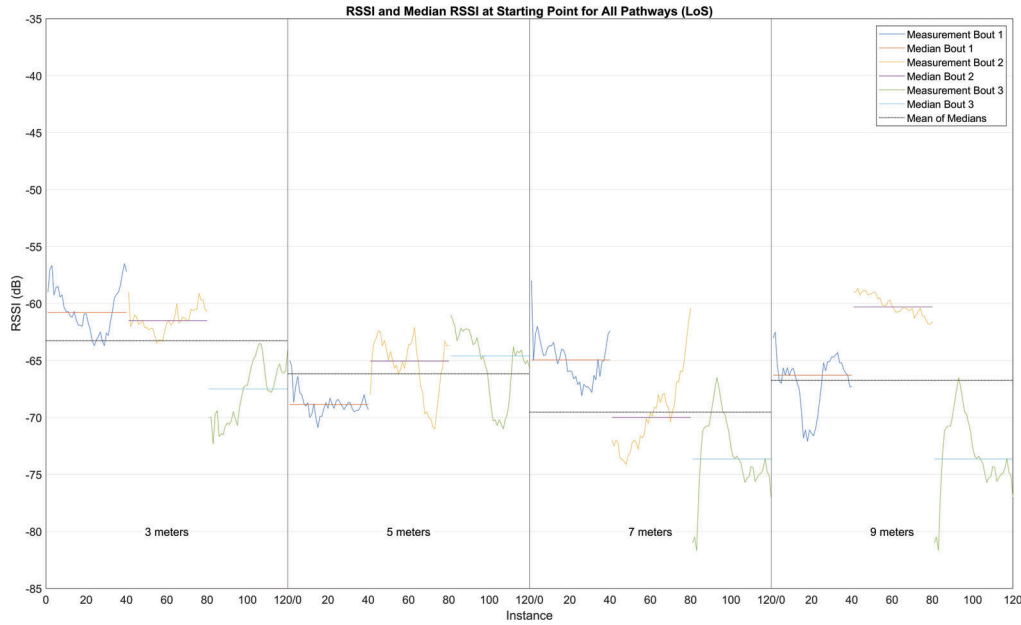


FIGURE 2.9: Comparison of RSSI and the Median Values for Three rounds of 1-minute at *Start* Location on All Pathways (LoS)

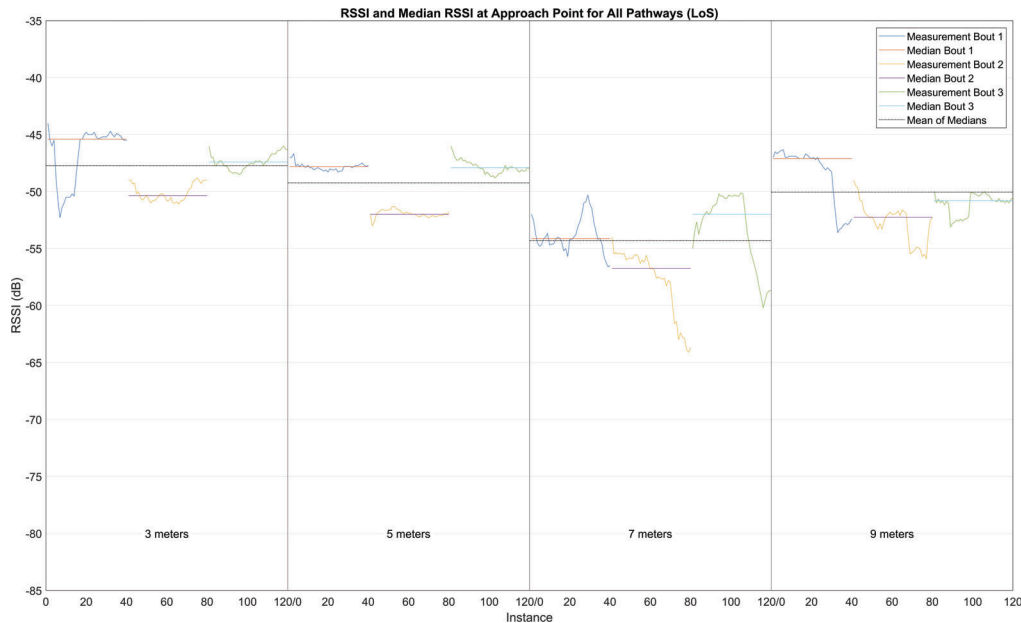


FIGURE 2.10: Comparison of RSSI and the Median Values for Three rounds of 1-minute at *Approach* Location on All Pathways (LoS)

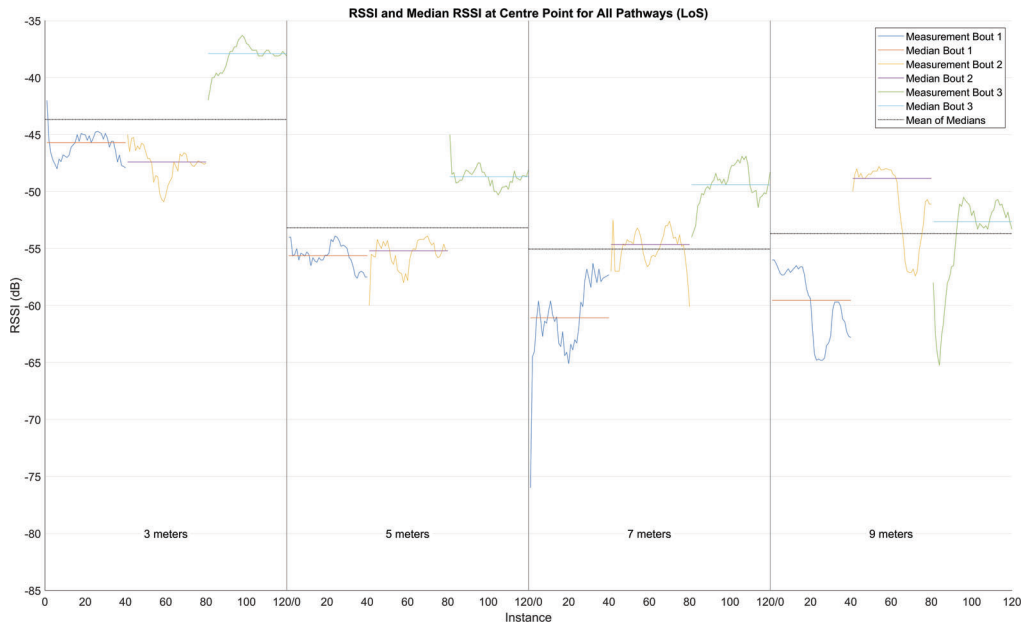


FIGURE 2.11: Comparison of RSSI and the Median Values for Three rounds of 1-minute at *Centre* Location on All Pathways (LoS)

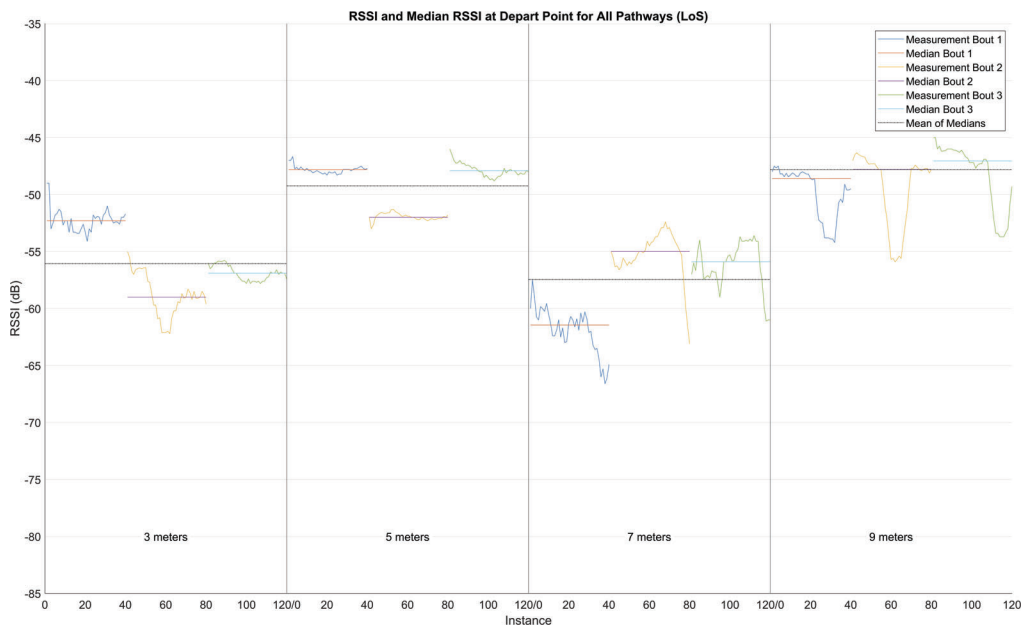


FIGURE 2.12: Comparison of RSSI and the Median Values for Three rounds of 1-minute at *Depart* Location on All Pathways (LoS)

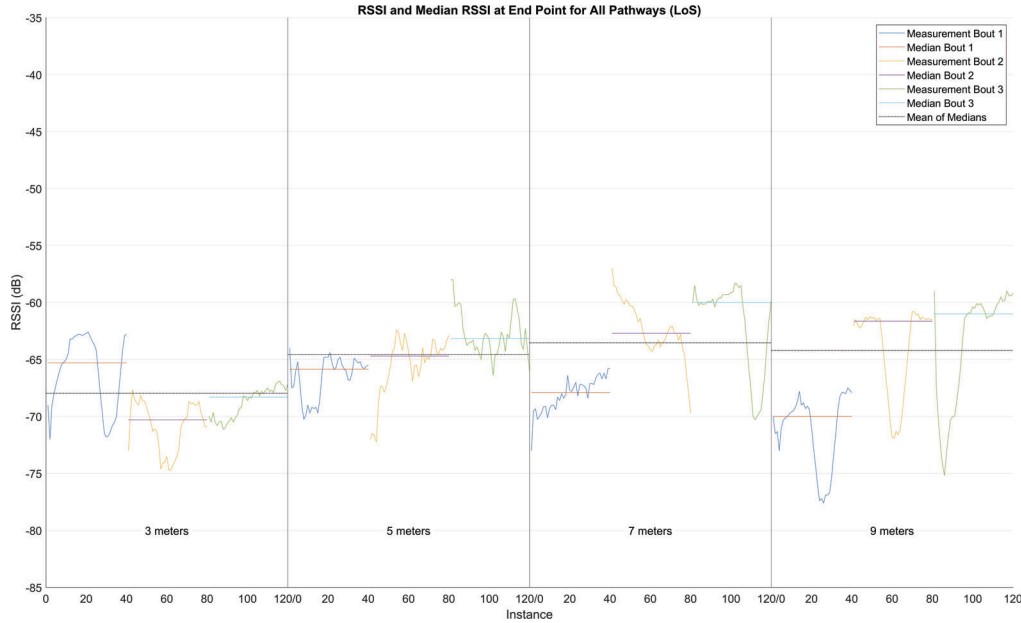


FIGURE 2.13: Comparison of RSSI and the Median Values for Three rounds of 1-minute at *End* Location on All Pathways (LoS)

Similarly, Figures 2.14, 2.15, 2.16, 2.17, and 2.18 depicts the captured RSS values at *start*, *approach*, *centre*, *depart*, and *end* locations respectively on each of the pathways with their own median values, and the mean of those median values in the case of nLoS.

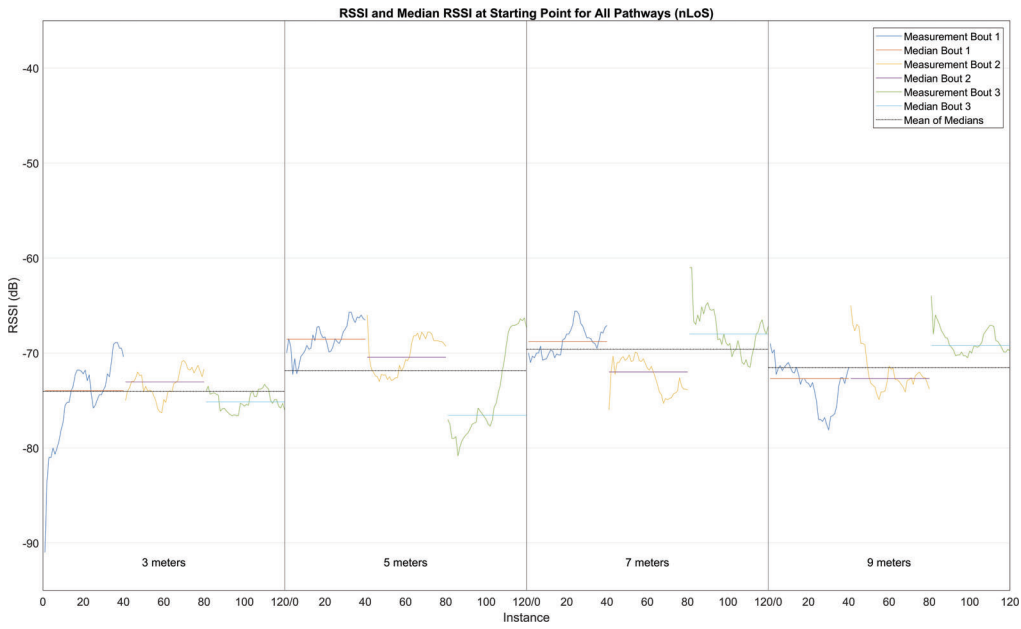


FIGURE 2.14: Comparison of RSSI and the Median Values for Three rounds of 1-minute at *Start* Location on All Pathways (nLoS)

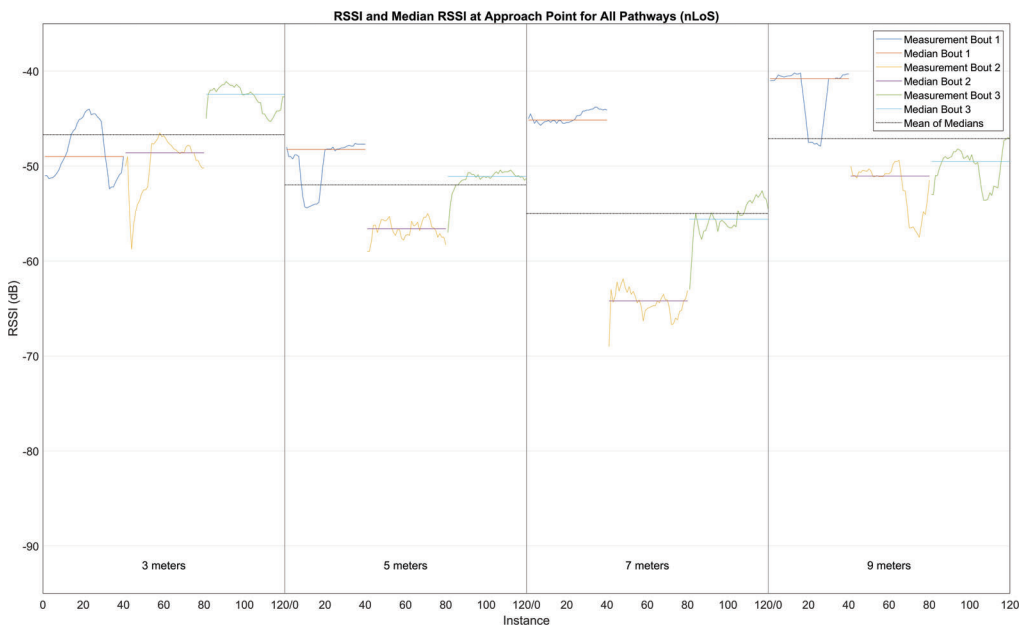


FIGURE 2.15: Comparison of RSSI and the Median Values for Three rounds of 1-minute at *Approach* Location on All Pathways (nLoS)

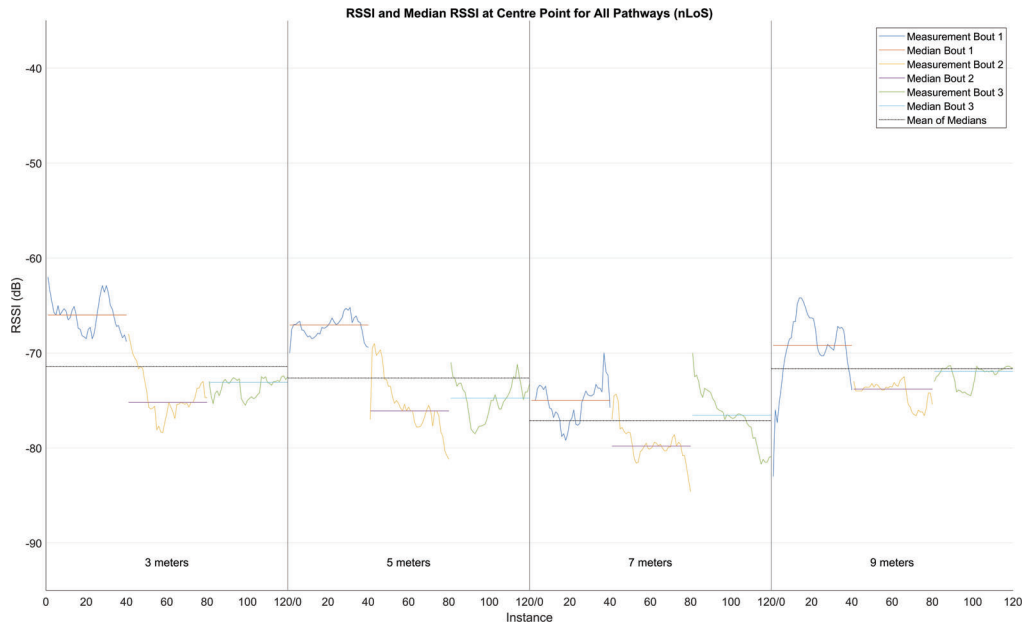


FIGURE 2.16: Comparison of RSSI and the Median Values for Three rounds of 1-minute at *Centre* Location on All Pathways (nLoS)

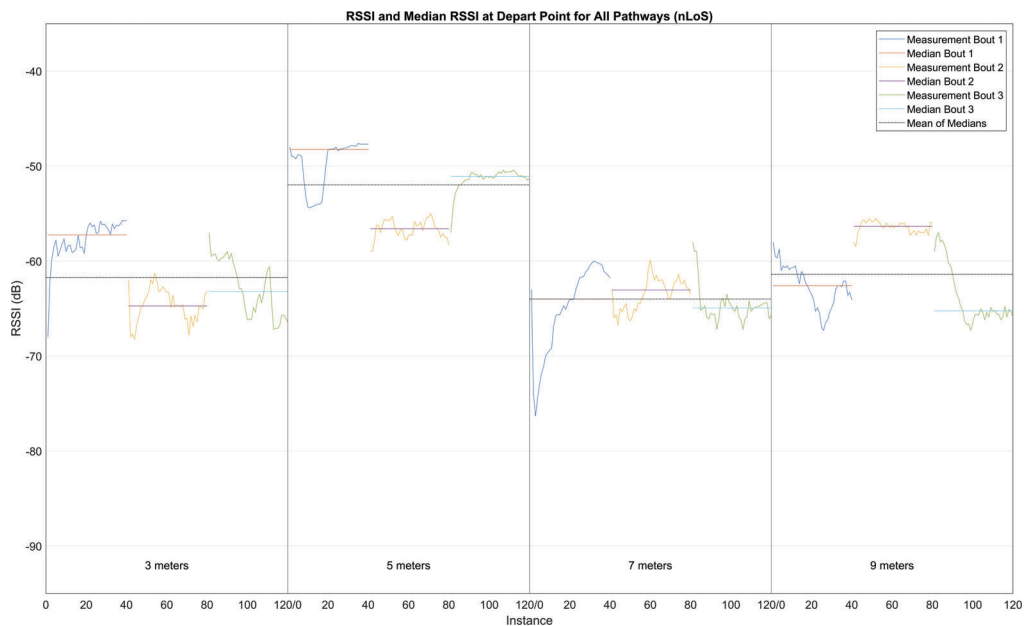


FIGURE 2.17: Comparison of RSSI and the Median Values for Three rounds of 1-minute at *Depart* Location on All Pathways (nLoS)

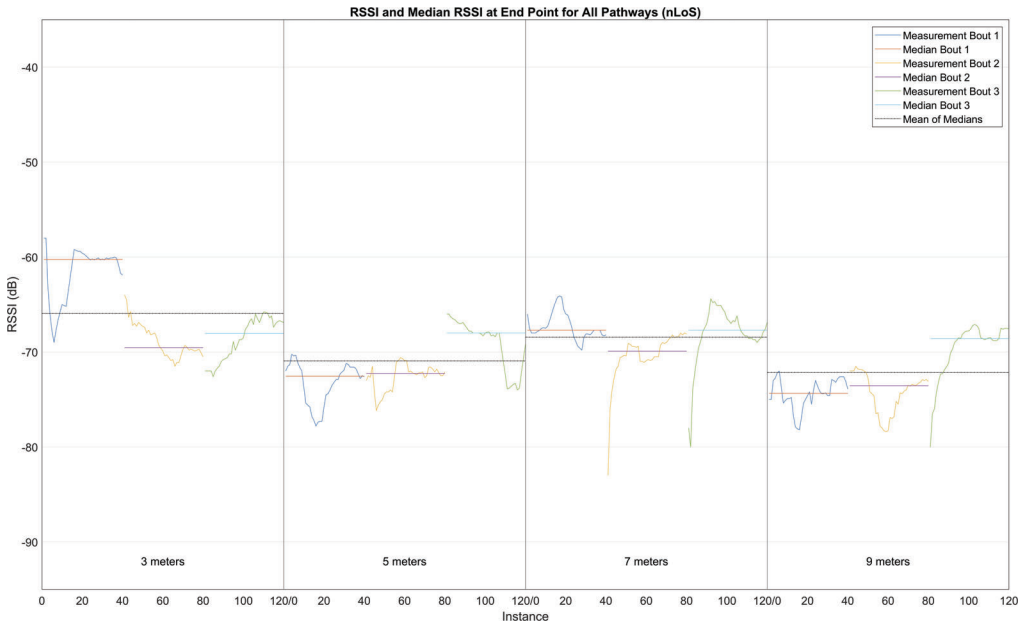


FIGURE 2.18: Comparison of RSSI and the Median Values for Three rounds of 1-minute at *End* Location on All Pathways (nLoS)

To detect the presence of any statistically significant differences in the measurements, the ANOVA technique, followed by Tukey's HSD post-hoc analysis was applied to the data. This technique was presented in subsection 1.4.7 of Chapter 1. To do this, the data from all the rounds for each location at each pathway were combined and used. The LoS and nLoS cases were separately analysed. While they could be combined to gain an overall understanding, they were analysed separately to see if any nuances could be discovered in the process. The result obtained from ANOVA for the LoS case is presented in Figure 2.19. The upper whisker and the lower whisker in the box plot depict the minimum and maximum RSSI respectively whereas the red line depicts the median value. The upper bound of the box represents the 75th percentile and the bottom represents the 25th percentile values. If the notches, which are at the 5% significance level, do not overlap with the notches of other groups, then the two medians are significantly different.

#### Quick Recap

**Confidence Interval (CI):** CI in ANOVA provides a range of values that likely contain population parameters such as a mean difference between the groups with a specified level of confidence, 95% in this case.

The results of ANOVA for the LoS case were fed into Tukey's HSD test. The outcome is presented in Table 2.5. The first two columns in the table represent a comparison of the two groups. The lower and upper bounds of CI are in rows three and five,

while the fourth column represents the difference in means of the two groups being compared. Finally, the sixth column represents the *p*-value. The CI represents the range of values where the difference of means is likely to fall. If the values of the lower and upper bound are such that they contain 0, that is if the intervals have opposite signs, it signifies that there is no statistically significant difference between the two groups. The *p*-value is the measure of the probability of obtaining extreme results on the assumption of the null hypothesis being true. In this case, the null hypothesis dictates that there is no significant difference between the two. The *p*-value is always compared against some threshold for significance,  $\alpha$ , which in this case is

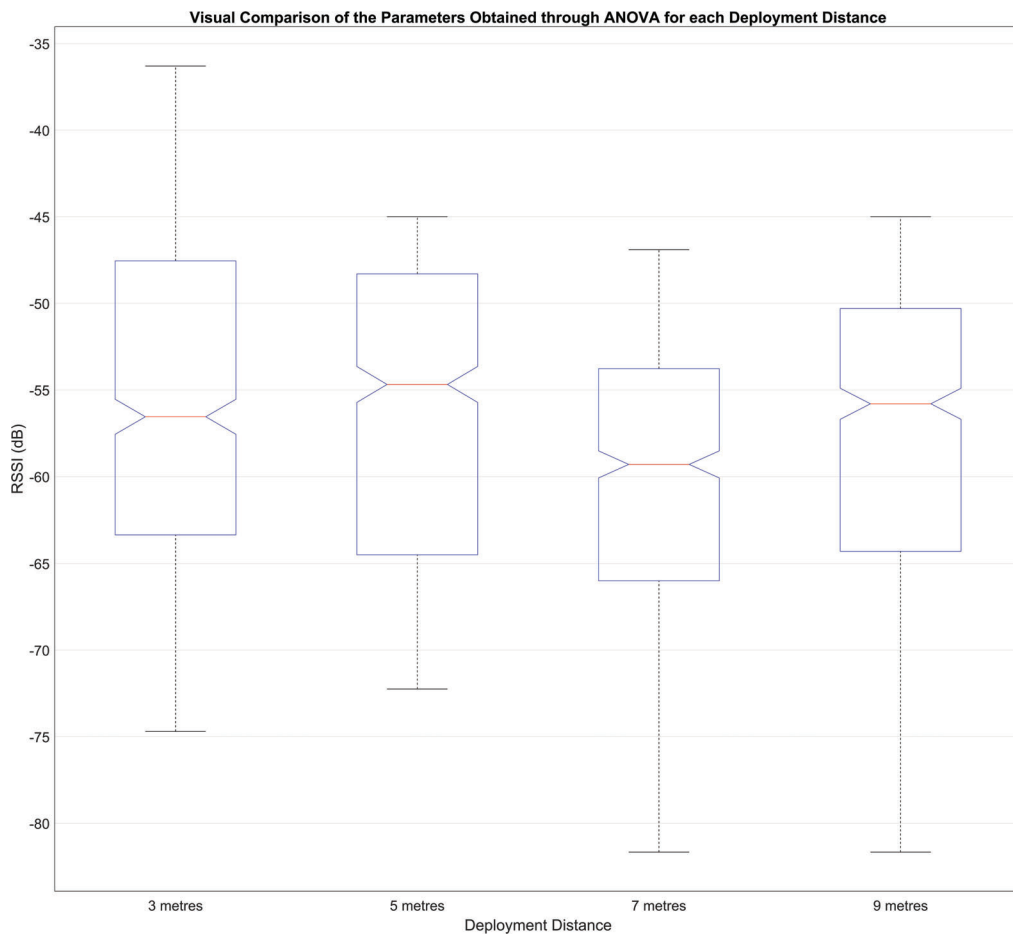


FIGURE 2.19: Results of ANOVA on LoS Measurements

0.05, as mentioned in Section 1.4.7 in Chapter 1. Therefore, if the  $p$ -value is greater than 0.05, then, the null hypothesis cannot be rejected. The outcome of Tukey's HSD test for the LoS case is also visualised in Figure 2.20. The error bars in the figure represent the CI with a marker at the difference of means. The dotted horizontal line represents the zero difference. The error bars, representing the CI passing over the zero difference line signifies that there is no statistically significant difference between the particular pair or group.

Group 1	Group 2	CI <sup>1</sup>	Lower Bound	Difference in Means	CI Upper Bound	$p$ -value
3m	5m		-0.6065	0.6817	1.9700	0.5249
3m	7m		2.6236	3.9119	5.2002	0
3m	9m		0.3530	1.6413	2.9296	0.0059
5m	7m		1.9419	3.2302	4.5185	0
5m	9m		-0.3288	0.9595	2.2478	0.2223
7m	9m		-3.5589	-2.2706	-0.9823	0

TABLE 2.5: Outcome of Tukey's HSD (LoS)

<sup>1</sup> CI is a range of values between which the difference in means is likely to be found.

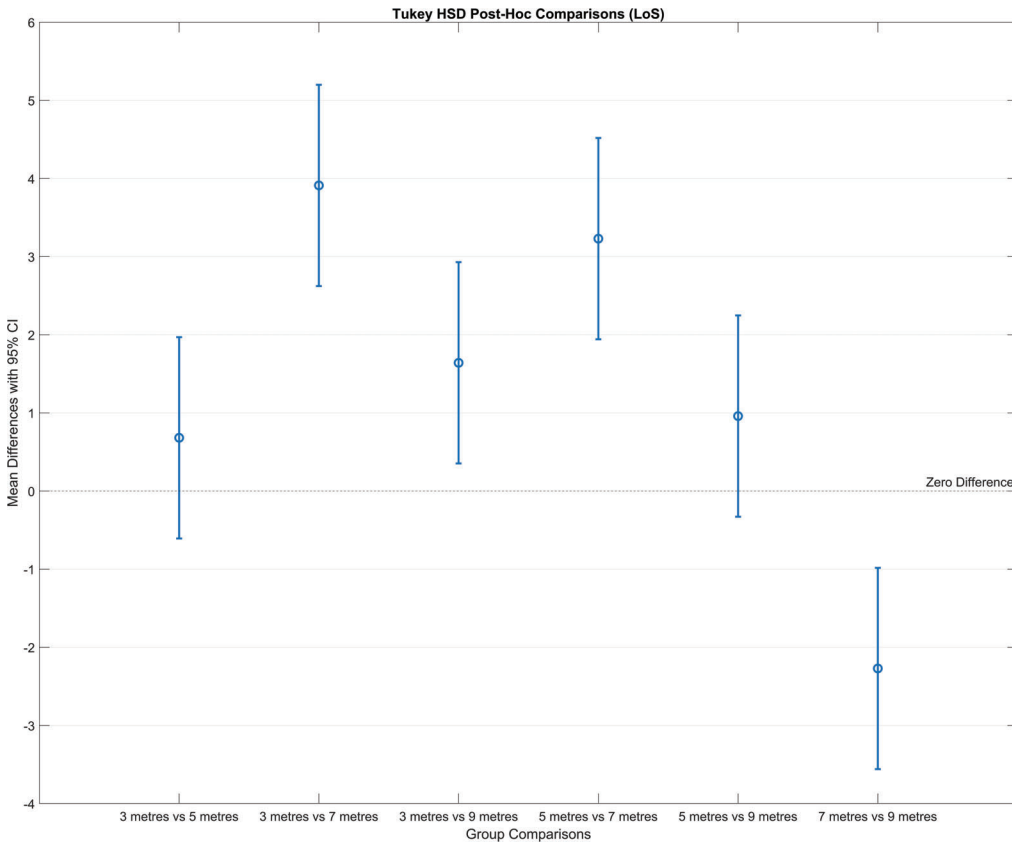


FIGURE 2.20: Comparison of CI, Median, and Zero Difference for Each Group of Deployment Distances (LoS)

The following findings, as presented in Table 2.5, were obtained from this analysis:

1. 3 metres vs 5 metres

- Lower bound of CI: -0.6065. Upper bound of CI: 1.97. Since this range contained 0, it indicated that there is no statistically significant difference in the means.
- The  $p$ -value is 0.5249, which was found to be greater than  $\alpha$ . Therefore, the null hypothesis was not rejected.
- **Verdict:** Based on the presence of 0 in the CI and high  $p$ -value, the difference in the means was not a true difference but likely to be a random variation. *No significant difference.*

#### 2. 3 metres vs 7 metres

- Lower bound of CI: 2.6236. Upper bound of CI: 5.2002. Since this range did not contain 0, it indicated that there was a statistically significant difference in the means.
- The  $p$ -value was 0, which was less than  $\alpha$ . Therefore, the null hypothesis was rejected.
- **Verdict:** Significant difference. 3 metres was better than 7 metres.

#### 3. 3 metres vs 9 metres

- Lower bound of CI: 0.3530. Upper bound of CI: 2.9296. Since this range did not contain 0, it indicated that there was a statistically significant difference in the means.
- The  $p$ -value was 0.0059, which was less than  $\alpha$ . Therefore, the null hypothesis was rejected.
- **Verdict:** Significant difference. 3 metres was better than 9 metres.

#### 4. 5 metres vs 7 metres

- Lower bound of CI: 1.9419. Upper bound of CI: 4.5185. Since this range did not contain 0, it indicated that there was a statistically significant difference in the means.
- The  $p$ -value was 0, which was less than  $\alpha$ . Therefore, the null hypothesis was rejected.
- **Verdict:** Significant difference. 5 metres was better than 7 metres.

#### 5. 5 metres vs 9 metres

- Lower bound of CI: -0.3288. Upper bound of CI: 2.2478. Since this range contained 0, it indicated that there was no statistically significant difference in the means.
- The  $p$ -value was 0.2223, which was greater than  $\alpha$ . Therefore, the null hypothesis was not rejected.
- **Verdict:** There was no significant difference.

#### 6. 7 metres vs 9 metres

- Lower bound of CI: -3.5589. Upper bound of CI: -0.9823. Since this range did not contain 0, it indicated that there was a statistically significant difference in the means.
- The  $p$ -value was 0, which was less than  $\alpha$ . Therefore, the null hypothesis was rejected.

- **Verdict:** Significant difference. 7 metres was better than 9 metres.

Based on these findings, the deployment distance of 3 metres consistently produced significantly higher mean results compared to 7 metres and 9 metres. However, the difference between 3 metres and 5 metres was not statistically significant. The deployment distance of 5 metres produced significantly higher results compared to 7 metres but did not differ significantly from 9 metres. Finally, the results for 7 metres were significantly higher than those for 9 metres.

Given these results, the most effective deployment distances appeared to be 3 metres and 5 metres, with no significant difference between them, suggesting that either could be optimal depending on the context or specific goals of the deployment. It is noteworthy that the distance in this regard is horizontal distance, and does not take into account the height at which it is deployed.

Results of ANOVA for the nLoS case are presented in Figure 2.21. Here, some outlier values can also be seen as red-coloured + symbols. The ANOVA result fed into Tukey's HSD produced the output presented in Table 2.6 and in Figure 2.22. The summary derived from these results is as follows:

#### 1. 3 metres vs 5 metres

- Lower bound of CI: -1.5304. Upper bound of CI: 1.3804. Since this range contained 0, it indicated that there was no statistically significant difference in the means.
- The  $p$ -value was 0.9992, which was greater than  $\alpha$ . Therefore, the null hypothesis was not rejected.
- **Verdict:** No significant difference.

#### 2. 3 metres vs 7 metres

- Lower bound of CI: 0.1637. Upper bound of CI: 3.0746. Since this range did not contain 0, it indicated that there was a statistically significant difference in the means.
- The  $p$ -value was 0.022, which was less than  $\alpha$ . Therefore, the null hypothesis was rejected.
- **Verdict:** Significant difference. 3 metres was better than 7 metres.

#### 3. 3 metres vs 9 metres

- Lower bound of CI: -0.5514. Upper bound of CI: 2.3594. The range contained 0, indicating no statistically significant difference in the means.
- The  $p$ -value was 0.3810, which was greater than  $\alpha$ . Therefore, the null hypothesis was not rejected.
- **Verdict:** No significant difference.

#### 4. 5 metres vs 7 metres

- Lower bound of CI: 0.2387. Upper bound of CI: 3.1495. Since this range did not contain 0, it indicated that there was a statistically significant difference in the means.

- The  $p$ -value was 0.0148, which was less than  $\alpha$ . Therefore, the null hypothesis was rejected.
- **Verdict:** *Significant difference.* 5 metres was better than 7 metres.

#### 5. 5 metres vs 9 metres

- Lower bound of CI: -0.4764. Upper bound of CI: 2.4344. Since this range contained 0, it indicated that there was no statistically significant difference in the means.
- The  $p$ -value was 0.3090, which was greater than  $\alpha$ . Therefore, the null hypothesis was not rejected.
- **Verdict:** *No significant difference.*

#### 6. 7 metres vs 9 metres

- Lower bound of CI: -2.1705. Upper bound of CI: 0.7403. The range contained 0, indicating no statistically significant difference in the means.
- The  $p$ -value was 0.5870, which was greater than  $\alpha$ . Therefore, the null hypothesis was not rejected.
- **Verdict:** *No significant difference.*

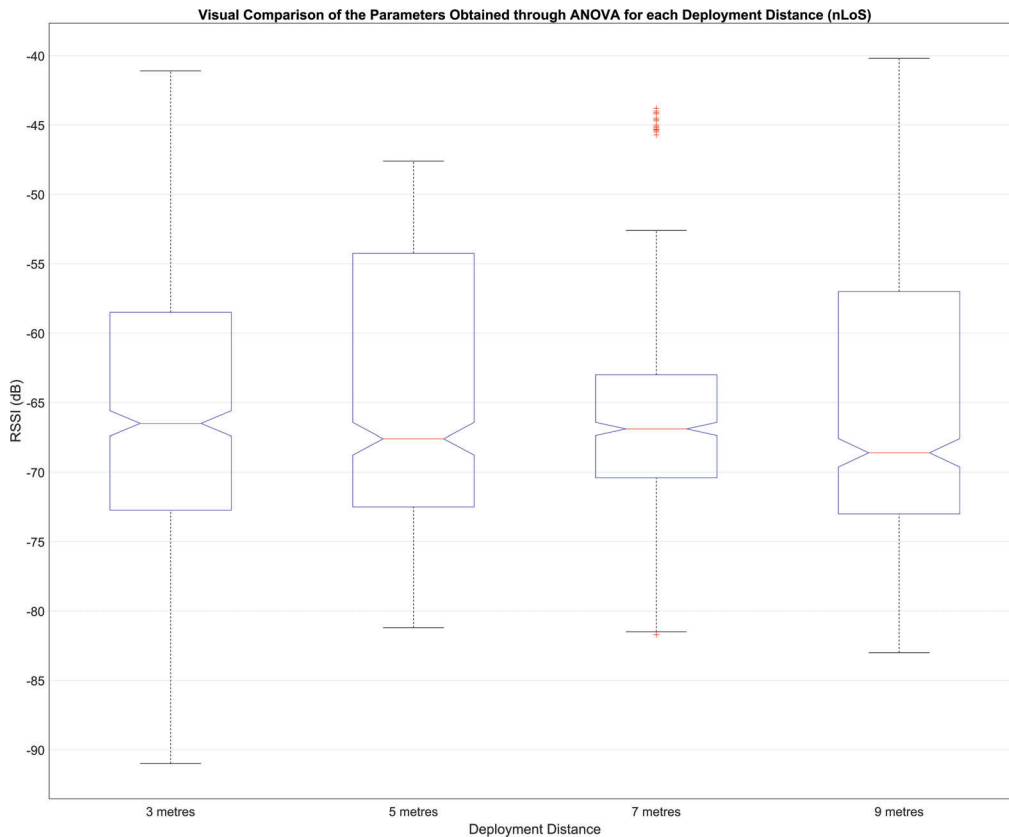


FIGURE 2.21: Results of ANOVA on nLoS Measurements

Through the results of ANOVA and Tukey's HSD tests, both 3 metres and 5 metres from the closest approach of a pedestrian appeared to be more suitable deployment

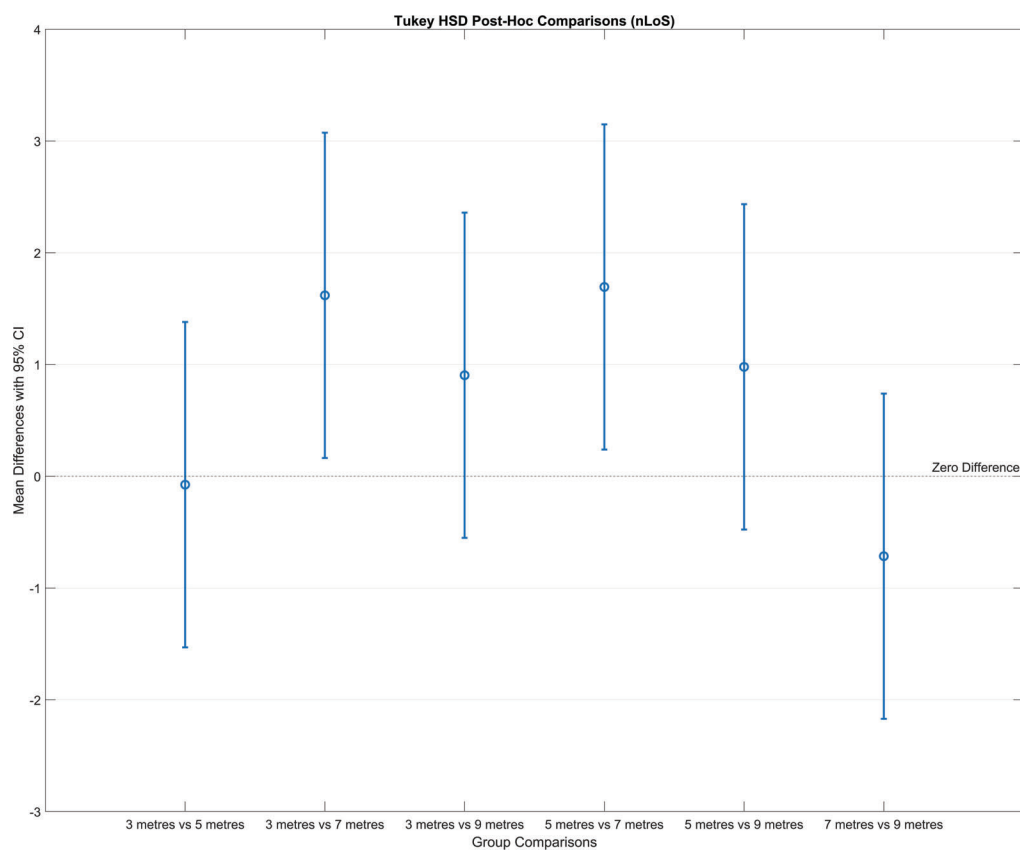


FIGURE 2.22: Comparison of CI, Median, and Zero Difference for Each Group of Deployment Distances (nLoS)

Group 1	Group 2	CI Lower Bound	Difference in Means	CI Upper Bound	p-value
3m	5m	-1.5304	-0.0750	1.3804	0.9992
3m	7m	0.1637	1.6191	3.0746	0.0222
3m	9m	-0.5514	0.9040	2.3594	0.3810
5m	7m	0.2387	1.6941	3.1495	0.0148
5m	9m	-0.4764	0.9790	2.4344	0.3090
7m	9m	-2.1705	-0.7151	0.7403	0.5870

TABLE 2.6: Outcome of Tukey's HSD (nLoS)

distances than the deployment distances of 7 *metres* and 9 *metres*. While the results obtained thus far were satisfactory to conclude that those deployment distances are superior, another statistical test was conducted to compare the two candidates, 3 *metres* and 5 *metres*, that were found to be more adequate than the others in the previous tests. To do this test, MDA, which is described in the Section 1.4.6 in Chapter 1, values were calculated for each of the locations on all pathways, combining measurements from all rounds.

#### Information

The *double hump* pattern is not investigated in the nLoS case because in that case, the RSS will always be lower at the *centre* point due to full occlusion by the body of the volunteer pedestrian, as seen in Figure 1.21.

Error bars were plotted to depict the deviations obtained from the MDA values and a marker was placed on the error bars to denote the median value. Lines were connected between the subsequent locations on the same deployment distances to represent a hypothetical progression trend in the RSS values. This is presented in Figure 2.23 for

the LoS case and in Figure 2.24 for the nLoS case. While the outcome did not provide any evidence of superior signal strength between 3 *metres* and 5 *metres* deployment distance, it highlighted another important fact. In the deployment distances of 5 *metres* and 9 *metres* for the LoS case, a *double hump* pattern similar to the one obtained in the anechoic chamber was observed. Now, it is noteworthy that the distance between the Observer and the Broadcaster in the anechoic chamber remained constant, whereas, in this experiment, the distances between the two devices increased in either direction along the pathway from the *centre* point. This presence of a double hump pattern despite varying distances on the linear pathway means that there is a likelihood of obtaining this feature during a walk by a pedestrian. Since this is a salient feature in the RSSI pattern when it appears, it can be used to assert information regarding the movement of the pedestrian as well. This will be revisited in Section 2.1.3 in this Chapter. Finally, the average of all the medians across the entire pathway was calculated and compared with other candidate deployment distances. The horizontal lines in Figure 2.25 and Figure 2.26 depict the average medians for entire pathways for the cases of LoS and nLoS respectively.

Finally, an assessment of fluctuations at each pathway was performed. This analysis of fluctuations provided an opportunity to identify the pathway that produced RSSI patterns that are more accurate representation of pedestrian's walk, that is they are less influenced by environmental topology. This analysis was performed by assessing the SS Fading through Rician distribution fitting, as mentioned in Section 1.3.2.2 in Chapter 1. The explanation behind the analysis was already described in Section 2.1.2 of this chapter, and the result for the deployment distance of 3 *metres* was also presented in the same section in Figure 2.6. Only LoS cases were considered for this analysis, as SS fading assesses the dominance of LoS component which will

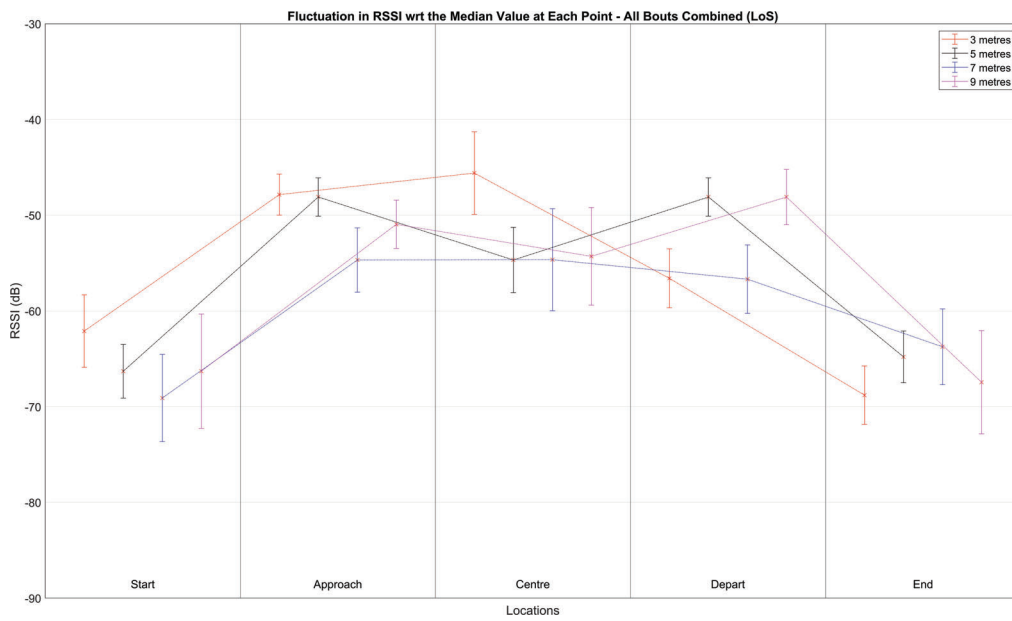


FIGURE 2.23: Comparison between Deviations in the RSS Values for All Deployment Distances at Each Key Point on the Pathway (LoS)

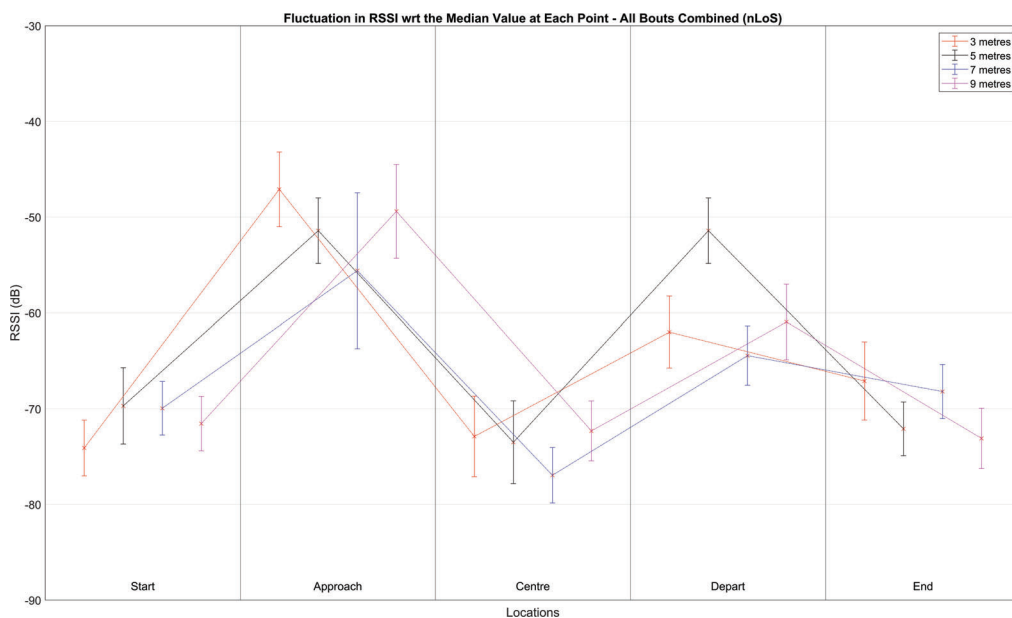


FIGURE 2.24: Comparison between Deviations in the RSS Values for All Deployment Distances at Each Key Point on the Pathway (nLoS)

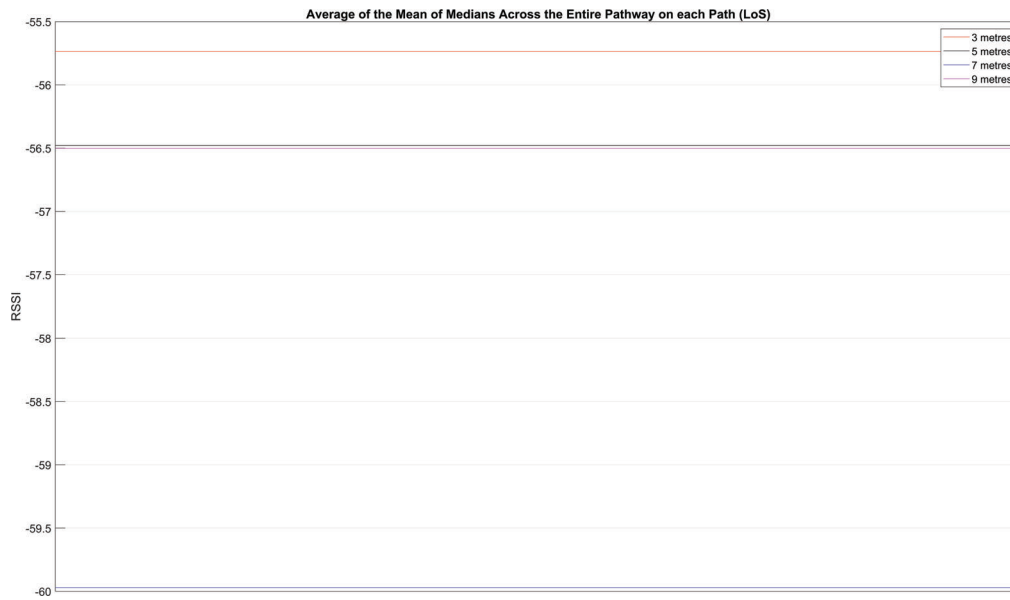


FIGURE 2.25: Average Median Across All Key Points on Each Pathway (LoS)

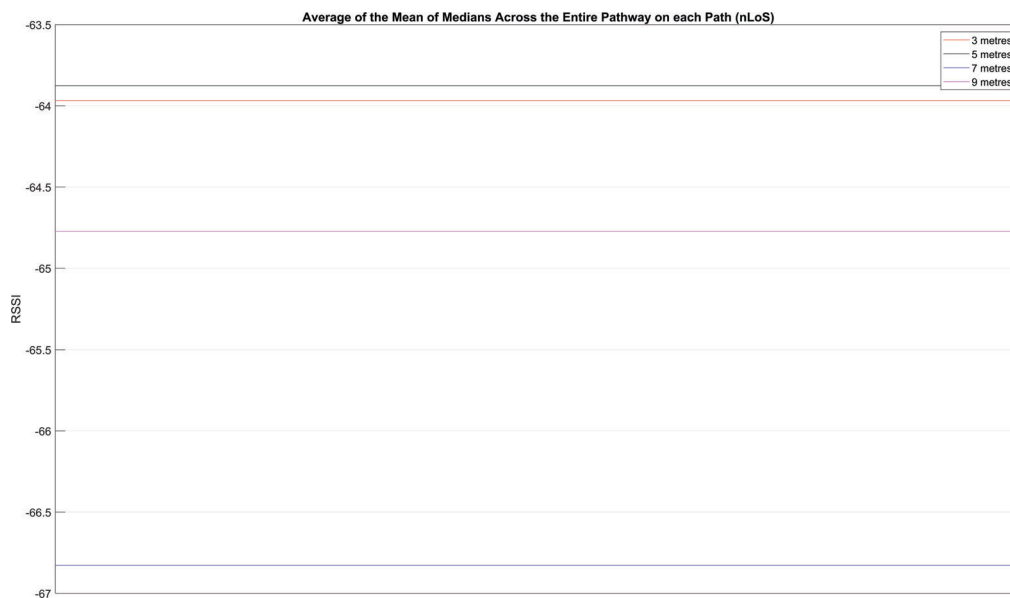


FIGURE 2.26: Average Median Across All Key Points on Each Pathway (nLoS)